Carrier injection from gold electrodes into thioacetyl-end-functionalized poly(*para*-phenyleneethynylene)s

Wenping Hu,* Hiroshi Nakashima, Kazuaki Furukawa, Yoshiaki Kashimura, Katsuhiro Ajito, Chunxi Han, and Keiichi Torimitsu

NTT Basic Research Laboratories, NTT Corporation, 3-1 Morinosato Wakamiya, Atsugi, Kanagawa 243-0198, Japan

(Received 15 December 2003; revised manuscript received 22 January 2004; published 21 April 2004)

Carrier injection from a gold electrode into a thioacetyl-end-functionalized polymer, poly(*para*-phenyleneethynylene)s (TA-PPE), has been investigated by using sandwich and nanogap electrode devices. The results suggest that carrier injection depends on the organized status of the Au/TA-PPE interface. For sandwich devices with spin-coated TA-PPE films, carrier injection is dominated by a thermal emission mechanism with a barrier height of around 1.16 eV. However, as regards devices with nanogap electrodes, when the Au/TA-PPE interface is poorly organized, the carrier injection is dominated by a mixed mechanism consisting of thermal emission and tunneling. When the Au/TA-PPE interface is well organized, i.e., most of the molecules are connected to the Au electrode by Au-S bonds, and the carrier injection is dominated by tunneling, the tunneling barrier height Φ_B is estimated to be around 1.33–1.43 eV.

DOI: 10.1103/PhysRevB.69.165207 PACS number(s): 73.61.Ph, 73.63.Rt

I. INTRODUCTION

Conjugated polymers have been attracting considerable attention since the 1990s[1–8] due to their wide range of applications in devices such as organic light-emitting diodes (OLEDs), solar cells, and field-effect transistors. Of these polymers (oligomers are not included here), poly(*para*-phenyleneethynylene)s (PPE) have provided many advantages for OLEDs and are regarded as good electroluminescent materials.[9–11] Moreover, the ideal rigidity of PPE molecules, which originates from the presence of the triple bond (which prevents the rotation of adjacent phenyl rings with respect to each other), gives the polymer many potential applications in nanotechnology (e.g., in nanowires).[12,13] Furthermore, by modifying PPE with thiol/thioacetyl-end-functionalized groups (so-called ''molecular alligator clips,'' which can adhere to Au electrodes[14,15] via Au-S bonds), there are good prospects for applying this thiol/thioacetyl-end-functionalized polymer to nano/molecular electronics. As regards devices constructed by self-assembly, impressive progress has been made on low molecular weight materials (e.g., conjugated phenylene ethynylene oligomers),[14,15] however, as far as we know no reports have dealt with the fabrication of nanojunctions with conjugated polymers, although the outstanding electronic-photonic properties of conjugated polymers have been well known since the 1990s.[1–9] Recently, we synthesized a thioacetyl-end-functionalized PPE [which we call TA-PPE, as shown in Fig. 1(a) by $M_w \approx 54\,000$, $M_w/M_n = 2.47$, calculated from M_n, the average $n \approx 73$, and the dispersion of n value was roughly estimated among 15–570].[16] Here, we report carrier injection from Au electrodes into TA-PPE based on a gold sandwich [Fig. 1(b)] and coplanar nanogap electrode devices [Fig. 1(c)]. We adopted coplanar nanogap electrodes here is because this nanogap structure is more accessible for the future self-assembly of TA-PPE into potential electronic devices.

II. EXPERIMENTS

We fabricated sandwich devices by vacuum depositing Ti/Au (5 nm/50 nm) on glass substrates, then spin coating TA-PPE (~100 nm) on the Au/glass substrates, and finally depositing the top Au electrodes. The area of the sandwich devices was around 4 mm^2. Au gap electrode structures were prepared by electron beam lithography on Ti-primed (~50 Å) oxidized silicon substrates (SiO_2:300 nm). The gap width of the electrodes was around 100 nm [Fig. 1(d)]. The nanogap electrodes were first cleaned successively with pure water, hot acetone, hot ammonia-hydrogen peroxide solution (ammonia:hydrogen oxide:water=1:1:5), pure water and pure ethanol. Then several drops of TA-PPE were deposited around the electrode tip positions, and finally the electrodes were dried in an N_2 chamber. We obtained scanning electron microscope (SEM) images of the nanogap electrodes with a Hitachi *S*-4300 SE (Japan), fluorescent images of self-assembled TA-PPE nanowires with a Nikon Microphot FXA. Current-voltage (*IV*) measurements of the devices were recorded with a Low Temperature BCT-21 MDC Probe Station (Nagase, Japan) and a Keithley 6430. All measurements were performed in a vacuum (2–3 Pa).

III. RESULTS AND DISCUSSION

Au (5.2 eV) electrodes have a high work function, and so the injection of electrons into PPE is negligible and we only observed the current caused by the hole injection. In fact, no electroluminescence was found in the sandwich devices in the −5–+5-V range. The typical current density-voltage curves (*JV*) of the sandwich devices are shown in Fig. 2(a). The obvious temperature dependence suggested the presence of a thermal activation process during the hole injection. Furthermore, when we analyzed the observed *JV* properties on the basis of the tunneling and space-charge-limited current models, they did not reveal any dependence on voltage or temperature. These results indicate that the electrons are caused by the thermal emission mechanism. Here we analyzed the *JV*s based on the thermal emission model, taking account of the barrier lowering due to the image force, or the Schottky effect.

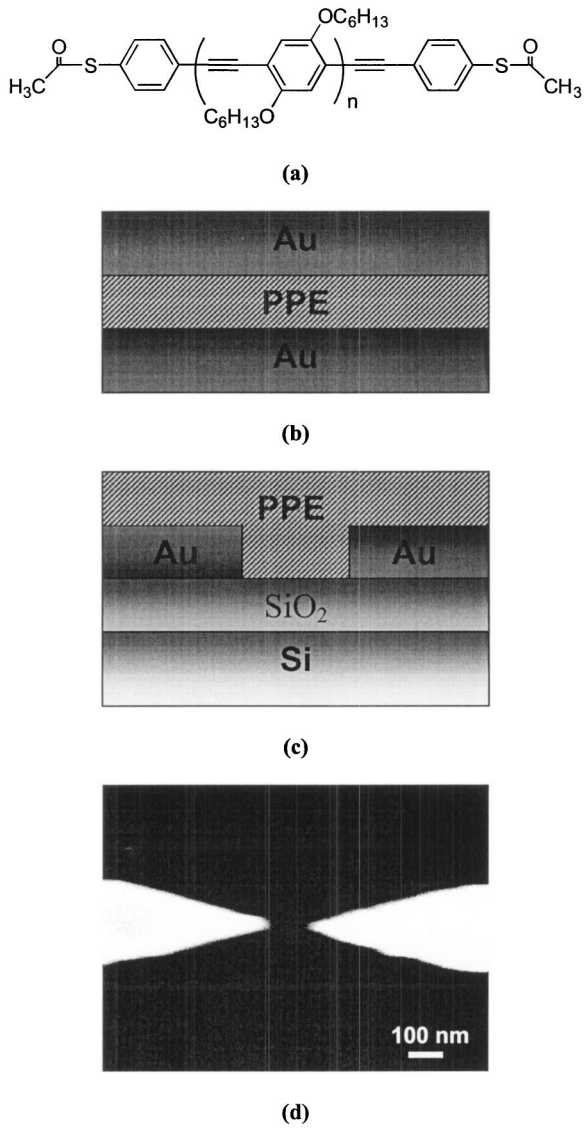

FIG. 1. (a) Molecular structure of thioacetyl-end-functionalized poly(*p*-phenyleneethynylene)s (TA-PPE). (b) Sandwich structures. (c) Nanogap electrode structures. (d) SEM image of the nanogap electrodes.

According to the thermal emission model the *JV* can be expressed as:[17,18]

$$J = A^* T^2 \exp\left[-\frac{\Phi_B - q\sqrt{qV/4\pi\varepsilon_0\varepsilon_r d}}{kT} \right],$$

where A^* is the effective Richardson constant, T is the temperature, $-\Phi_B$ is the barrier height at the interface, q is the electron charge, k is the Planck constant, ε_r is the dielectric constant of TA-PPE, ε_0 is the permittivity in a vacuum, and d is the TA-PPE thickness. In Fig. 2(b) the results of Fig. 2(a) are plotted to show the relationship between $\ln(J)$ and V. The extrapolated value of current density to zero voltage gives the saturation current density J_S, the barrier height can be obtained from the plot of $\ln(J_S/T^2) \propto T^{-1}$ as shown in Fig. 2(c), and the slope gives a barrier height of 1.16 eV. The barrier height obtained in our experiments agrees well with

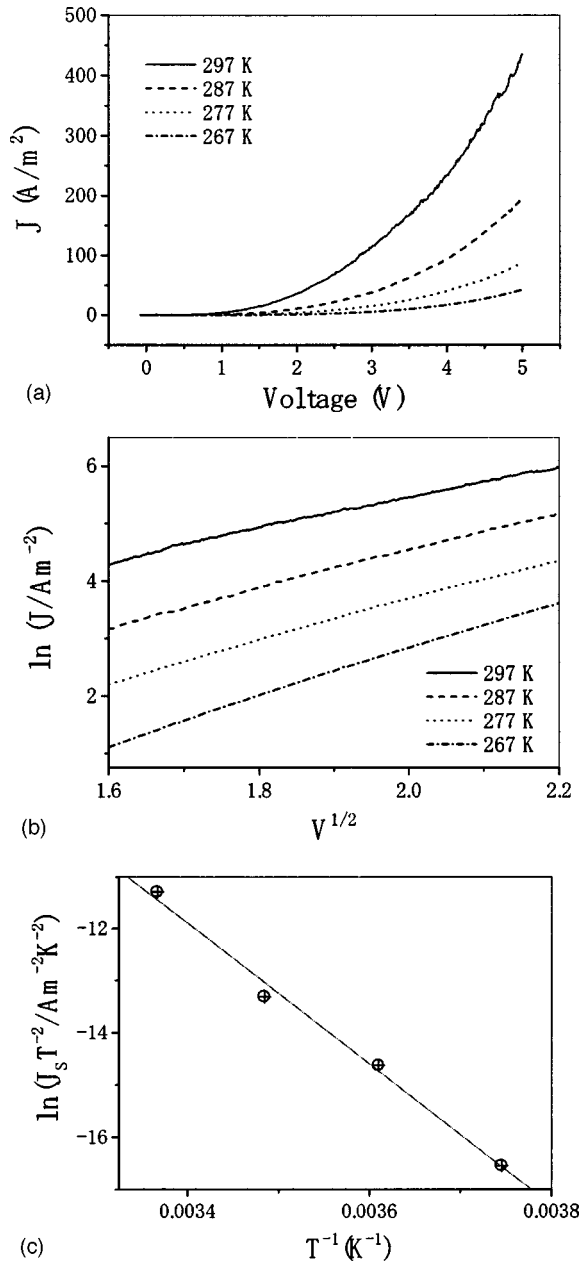

FIG. 2. (a) JV characteristics of sandwich devices consisting of Au/TA-PPE (100 nm)/Au/glass at different temperature. (b) $\ln J \sim V^{1/2}$ relationship of the data of (a), (c) $\ln(JT^{-2}) \sim 1/T$ relationship for the sandwich devices.

Weder *et al.*'s results.[19] They used ultraviolet photoelectron spectroscopy to determine that the ionization potential of poly(*p*-phenylene ethynylenes) is around 6.3 eV. If we assume that the work function of Au is about 5.2 eV, then the Au/PPE barrier height is around ~1.10 eV.[19]

As regards the devices with nanogap electrodes [Fig. 1(c)], the typical *JV*s of devices with new cast films are shown in Fig. 3. With respect to the coplanar geometry, the current transport between the two electrodes flows along a thin surface layer of unknown thickness. As a consequence of this two-dimensional geometry the current density is expressed in units of [A/m] instead of [A/m^2] for sandwiched electrodes.[20] Two features are clear in Fig. 3: (i) temperature

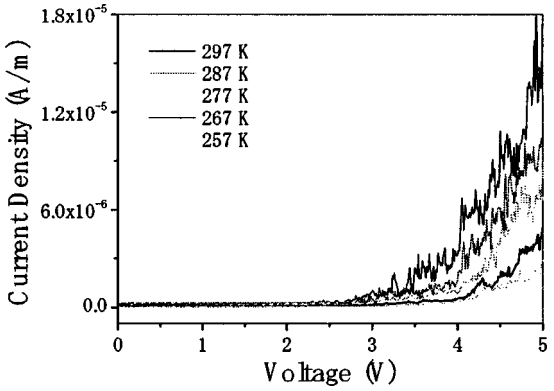

FIG. 3. JV characteristics of the gap electrode device with a new cast TA-PPE film.

dependence is still present; and (ii) there are some nonlinearly stepwise characteristics. The temperature dependence suggests the continued existence of the thermal activation process during hole injection. However, the nonlinearly stepwise characteristics are probably due to the tunneling injection.[21–35] In fact, when we analyzed the data in Fig. 3 by using $\ln J \propto V^{1/2}$ or an Arrhenius plot ($\ln J$ vs $1/T$), they did not fit either curve well. Therefore, it is probable that the hole injection is the result of a mixed mechanism in this case.

It is well known that thiol/thioacetyl-end-functionalized groups can act as ''molecular alligator clips'' to adhere to Au electrodes via Au-S bonds. Carrier injection through bonds is usually the result of a tunneling mechanism.[21–23,33,36–46] Here, although our TA-PPE possesses thioacetyl-functional end groups, the demonstration of temperature dependence in Figs. 2(a) and 3 suggests that the interface connection between the Au electrodes and TA-PPE is not realized by Au-S bonds, i.e., at this time, the Au/TA-PPE interface is not well organized. One possible reason for this poor organization is the rapid volatilization of the tetrahydrofuran (THF) solvent for the dropped and spin-coated films, which would mean that the TA-PPE molecules have insufficient time to rearrange themselves at the Au/TA-PPE interface.

In order to clarify this we placed the sample described in Fig. 3 in THF vapor (in a bottle 1/3 filled with THF) for another 96-h treatment. Moreover, methods have been described whereby NH_4OH promoted the deprotection of acetyl-protected thiols.[14,47–51] Therefore, a 20-ml ammonia solution was added to the THF solvents to generate a mixed THF/ammonia atmosphere to promote Au-TA-PPE connection. After this treatment, the samples were kept in a vacuum chamber for 24 h. Typical *JV*s of the treated samples are shown in Fig. 4(a): (i) the current density is much larger than that of the above untreated devices (as shown in Fig. 3); (ii) the temperature dependence is unclear; and (iii) nonlinearly stepwise characteristics are clear when the bias is changed, an example of which is shown in Fig. 4(b). The much improved current density suggested two possibilities: (1) improved hole injection, i.e., an improved interface between the TA-PPE and the Au electrodes, and (2) a transformation of the bulk TA-PPE between the nanogap electrodes. However, when we changed the electrodes from Au- to Pt (TA-PPE

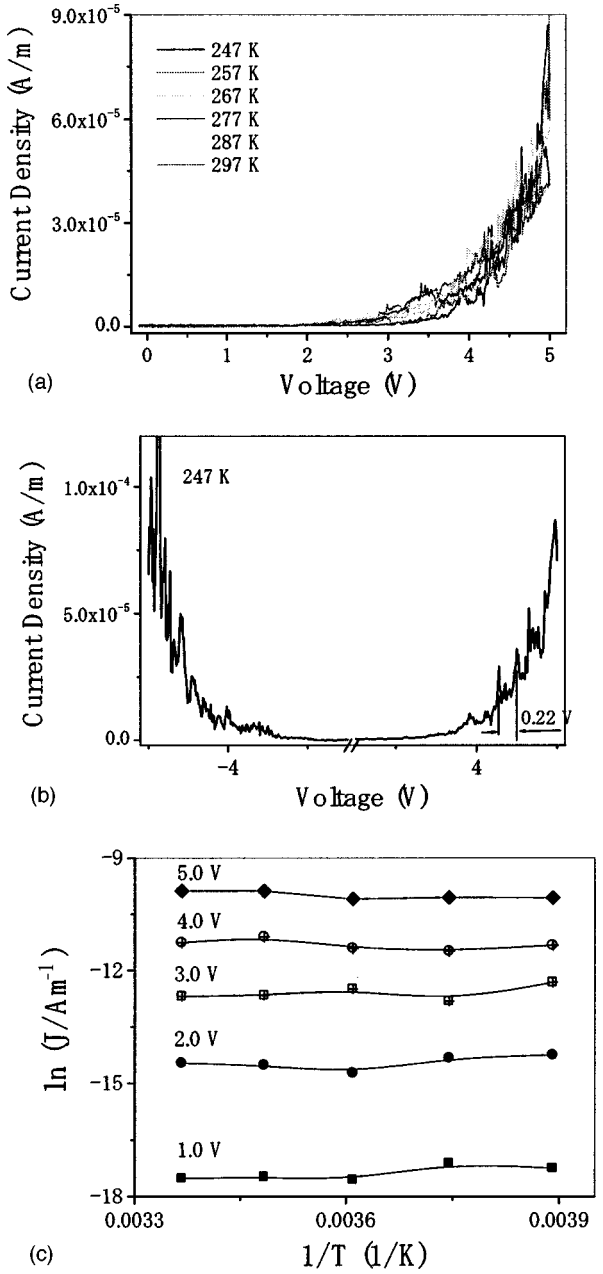

FIG. 4. (a) JV characteristics of Fig. 3 is device after being treated in an ammonia/THF atmosphere for 96 h. (b) JV characteristics of the device of (a) measured at 247 K. (c) $\ln J \sim 1/T$ relationship of the device of (a), suggesting no temperature dependence.

exhibits very weak adhesion on a Pt surface[16]), before and after the same ammonia/THF treatment, the current densities of the device showed no obvious change, which indicated that the effect of ammonia/THF on the bulk TA-PPE is not the key to the improved current density as shown in Fig. 4(a). That is, the much improved current density is very likely due to the improved Au/TA-PPE interface. Moreover, the fact that there is no significant temperature dependence in Fig. 4(a) proved that there is a much weaker thermal activation process in the hole injection. An Arrhenius plot ($\ln J$ vs $1/T$) of Fig. 4(a) is shown in Fig. 4(c) and it exhibits no significant temperature dependence in the $\ln J \sim 1/T$ slope at

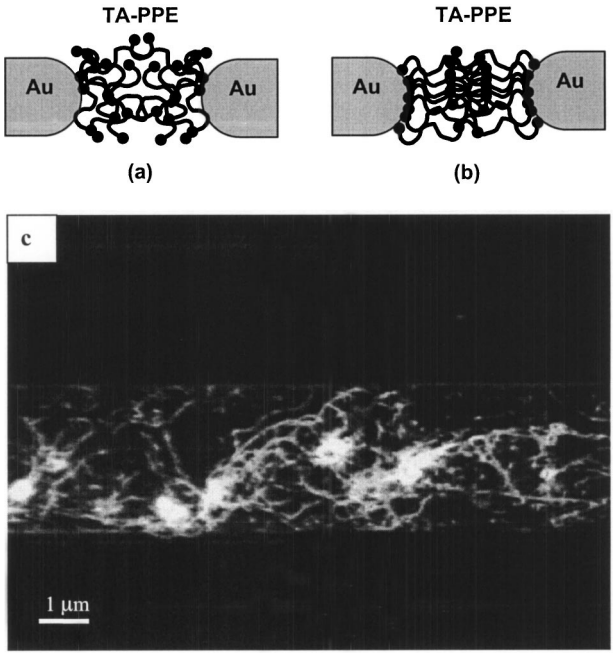

FIG. 5. (a) Au and TA-PPE connected model for the device with new cast polymer films. (b) Au and TA-PPE connected model for the device of (a) after being treated in an ammonia/THF atmosphere for 96 h. (c) Fluorescent image of self-assembled TA-PPE on a Au striped SiO_2 substrate.

different biases, which certainly reveals the absence of thermal activation in the sample after ammonia/THF treatment. The above two points enabled us to conclude that the hole injection is now dominated by tunneling.

With respect to the new spin-coated and dropped TA-PPE film on a Au substrate, the SEM results (not shown here) indicate that the film is amorphous. Therefore, it is reasonable to assume that the new dropped TA-PPE films, which came into contact with our nanogap electrodes, are also amorphous as shown in Fig. 5(a), because of the rapid volatilization of the THF solvent (the TA-PPE molecules have insufficient time to rearrange themselves). However, once the sample has again been treated in an ammonia-THF atmosphere for 96 h, the Au-TA-PPE connection at the Au/TA-PPE interface will be much improved [Fig. 5(b)] because of the fact that thiol/thioacetyl-functionalized-end groups can graft to Au surfaces. The connectivity between Au and our TA-PPE molecules has been identified by the absorption spectrum of TA-PPE on a Au substrate[16] and the self-assembled TA-PPE nanowires on Au substrates.[52] As a supplementary proof, the connectivity can be further enhanced as shown in Fig. 5(c). In this case, a SiO_2 substrate with a gold stripe is used for the experiments. The substrates were first cleaned successively with pure water, hot acetone, hot ammonia-hydrogen peroxide solution (ammonia:hydrogen oxide:water=1:1:5), pure water and pure ethanol. Then the substrates were dipped into an ammonia/TA-PPE solution for 96 h (TA-PPE concentration: 10^{-6} M; solvent: THF). Finally, the substrates were removed from the solution and cleaned gently, again with THF and pure water. It is interesting that the TA-PPE molecules

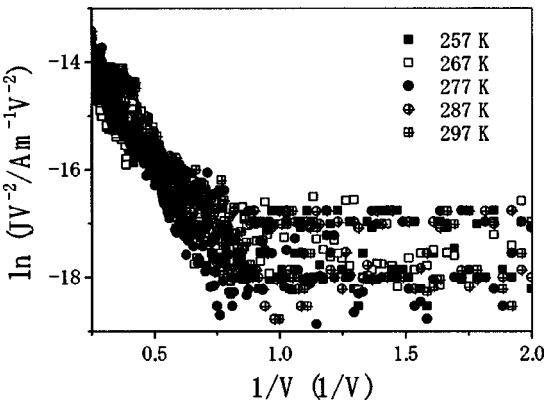

FIG. 6. $\ln JV^{-2} \sim 1/V$ relationship of the results in Fig. 4(a).

are adsorbed on the Au surfaces but not on the SiO_2 surfaces, demonstrating the good connectivity of Au-TA-PPE. This good connectivity is because ''molecular alligator clips'' have a strong affinity to Au surfaces, but a weak affinity to SiO_2 surfaces.

The above results further demonstrated the ideal connectivity between Au and our TA-PPE molecules if the polymer molecules have enough time to rearrange themselves in an ammonia/THF atmosphere, i.e., the correctness of the assumption of Fig. 5(b). However, we do not know whether the connected TA-PPE molecules are with or without alkyl-protected end groups, because no proof can suggest the complete deprotection of the alkyl end groups.

We assume that the carrier injection in our gap structures is ''through Au-S bond'' tunneling. The tunneling can be divided into direct tunneling (when $V \leqslant \Phi_B/e$) and Fowler-Nordheim tunneling (when $V \geqslant \Phi_B/e$). These two tunneling mechanisms can be distinguished by their distinct voltage dependence as shown in the following equations:[17,53]

$$J \propto V \exp\left[-\frac{2w\sqrt{2m\Phi_B}}{\hbar}\right]$$

(direct tunneling at $V < \Phi_B/e$),

$$J \propto V^2 \exp\left[-\frac{4w\sqrt{2m}}{3q\hbar V}(q\Phi_B)^{3/2}\right]$$

(Fowler-Nordheim tunneling at $V > \Phi_B/e$).

Here, w is the gap width of the electrodes, m is the effective mass of holes, $\hbar$ is Planck's constant, and Φ_B is the tunneling barrier height. We plot the results of Fig. 4(a) with a $\ln(J/V^2)$ vs $1/V$ in Fig. 6. It is clear that all the curves can be divided into two parts. In a low bias range ($1/V > 0.75$), the curves of $\ln(J/V^2)$ vs $1/V$ show no significant voltage dependence; in a high bias range ($1/V < 0.75$), the $\ln(J/V^2)$ vs $1/V$ curves exhibit similar linear relationships. The results indicate that carrier injection is dominated by Fowler-Nordheim tunneling at a high bias and by direct tunneling at a low bias. The dividing point is around $1/V \approx 0.7-0.75$. Therefore, it is reasonable to deduce that the tunneling barrier height of the Au-S bond Φ_B is around 1.33–1.43 eV. The result agrees well with

those of Reed *et al.*[53] They found that the Au-S tunneling barrier is around 1.39 ± 0.01 eV by studying the alkanethiol monolayer.

Our nanogap electrodes devices can be regarded as metal-molecule-metal (MMM) junctions, and many tunneling models have been proposed to describe the electronic transport through such MMM junctions.[36–46,53–58] For example, the Franz two-band model[53–56] was assumed to be useful for interpreting the electron transport through a molecular system with highest occupied molecular orbital and lowest unoccupied molecular orbital energy levels. Conjugated polymers are such molecular systems and they can be depicted by a typical energy band model. The Franz two-band model will probably be helpful in interpreting our MMM junctions. Moreover, because the geometry of the orbitals on the sulfurs does not permit the conjugated π orbitals from the TA-PPE molecules to interact strongly with the conduction orbitals of the gold electrodes, the mismatch of orbitals creates a potential barrier at each connection interface of the gap structure devices. This means a nanogap device is similar to a quantum dot junction, if we regard the conjugated TA-PPE molecules as quantum dots, with the terminal sulfur atoms acting as two tunnel barriers. The electron transport through the MMM junction is process sequential tunneling or resonant tunneling through double barriers. We anticipate that future researches, e.g., low temperature *JV* characteristics, will further clarify the tunneling model of electron transport through our MMM junction.

IV. CONCLUSION

In summary, carrier injection from gold into TA-PPE depends on the organization status of the Au/TA-PPE interface. In sandwich devices with spin-coated TA-PPE films the carrier injection is dominated by a thermal emission mechanism with a barrier height of around 1.16 eV. In nanogap electrode devices, carrier injection for devices with new cast films is dominated by a mixture mechanism of thermal emission and tunneling, because the rapid volatilization of the solvent (THF) results in a poorly organized Au/TA-PPE interface (TA-PPE molecules have insufficient time to rearrange themselves). However, after subjecting the sample to an ammonia/THF atmosphere for 96 h to reconstruct the Au/TA-PPE interface, i.e., to form a well-organized interface by means of the Au-S bond connection, the carrier injection is dominated by tunneling. The tunneling barrier height Φ_B is estimated to be around 1.33–1.43 eV.

ACKNOWLEDGMENTS

The authors are grateful to Dr. H. Takayanagi, Dr. H. Tamura, and Dr. H. Inokawa for provocative discussions.

*Author to whom correspondence should be addressed. Electronic address: huwp@iccas.ac.cn

[1] J. H. Burroughes, D. D. C. Bradley, A. R. Brown, R. N. Marks, K. Mackay, R. H. Friend, P. L. Burns, and A. B. Holmes, Nature (London) **347**, 539 (1990).
[2] G. Gustafsson, Y. Cao, G. M. Treacy, F. Klavetter, N. Colaneri, and A. J. Heeger, Nature (London) **357**, 477 (1992).
[3] B. J. Schwartz, M. R. Andersson, Q. Pei, and A. J. Heeger, Science **273**, 1833 (1996).
[4] H. Sirringhaus, N. Tessler, and R. H. Friend, Science **280**, 1741 (1998).
[5] R. H. Friend, R. W. Gymer, A. B. Holmes, J. H. Burroughes, R. N. Marks, C. Taliani, D. D. C. Bradley, D. A. Dossantos, J. L. Brédas, M. Lögdlund, and W. R. Salaneck, Nature (London) **397**, 121 (1999).
[6] H. Sirringhaus, P. J. Brown, R. H. Friend, M. M. Nielsen, K. Bechgaard, B. M. W. Langeveldvoss, A. J. H. Spiering, R. A. J. Janssen, E. W. Meijer, P. Herwig, and D. M. deLeeuw, Nature (London) **401**, 685 (1999).
[7] Y. Cao, I. D. Parker, G. Yu, C. Zhang, and A. J. Heeger, Nature (London) **397**, 414 (1999).
[8] N. Stutzmann, R. H. Friend, and H. Sirringhaus, Science **299**, 1881 (2003).
[9] U. H. Bunz, Chem. Rev. (Washington, D.C.) **100**, 1605 (2000).
[10] Q. Chu and Y. Pang, Macromolecules **36**, 4614 (2003).
[11] R. Dhirani, W. Zehner, R. P. Hsung, and P. Guyot-Sionnest, and L. R. Sita, J. Am. Chem. Soc. **118**, 3319 (1996).
[12] P. Samori, I. Sikharulidze, V. Francke, K. Muellen, and J. P. Rabe, Nanotechnology **10**, 77 (1999).
[13] P. Samori, N. Severin, K. Muellen, and J. P. Rabe, Adv. Mater. (Weinheim, Ger.) **12**, 579 (2000).
[14] J. M. Tour, L. Jones II, D. L. Pearson, J. J. S. Lamba, T. P. Burgin, G. M. Whitesides, D. L. Allara, A. N. Parikh, and S. V. Atre, J. Am. Chem. Soc. **117**, 9529 (1995).
[15] J. M. Tour, Chem. Rev. (Washington, D.C.) **96**, 537 (1996).
[16] H. Nakashima, K. Furukawa, Y. Kashimura, and K. Torimitsu, Polymer Preprints **44**, 482 (2003).
[17] S. M. Sze, *Physics of Semiconductor Devices*, 2nd ed. (Wiley, New York, 1981), Chap. 7.
[18] M. Matsumura and Y. Jinde, Appl. Phys. Lett. **73**, 2872 (1998).
[19] C. Weder, A. Montali, and P. Smith, Synth. Met. **97**, 123 (1998).
[20] J. A. Geust, Phys. Status Solidi **15**, 107 (1966).
[21] M. A. Reed, C. Zhou, C. J. Muller, T. P. Burgin, and J. M. Tour, Science **278**, 252 (1997).
[22] S. Hong, R. Reifenberger, W. Tian, S. Datta, J. Henderson, and C. P. Kubiak, Superlat. Microstruct. **28**, 289 (2000).
[23] D. J. Wold and C. D. Frisbie, J. Am. Chem. Soc. **123**, 5549 (2001).
[24] R. P. Andres, T. Bein, M. Dorogi, S. Feng, J. I. Henderson, C. P. Kubiak, W. Mahoney, R. G. Osifchin, and R. Reifenberger, Science **272**, 1323 (1996).
[25] S. Chen, R. S. Ingram, M. J. Hostetler, J. J. Pietron, R. W. Murray, T. G. Schaaff, J. T. Khoury, M. M. Alvarez, and R. L. Whetten, Science **280**, 2098 (1998).
[26] R. Wilkins, E. B. Jacob, and R. C. Jaklevic, Phys. Rev. Lett. **63**, 801 (1989).
[27] H. Ohnishi, Y. Kondo, and K. Takayanagi, Nature (London) **395**, 780 (1998).
[28] U. Banin, Y. Cao, D. Katz, and O. Millo, Nature (London) **400**, 542 (1999).
[29] M. T. Woodside and P. L. McEuen, Science **296**, 1098 (2002).
[30] H. Nejoh, Nature (London) **353**, 640 (1991).
[31] J. Chen, M. A. Reed, A. M. Rawlett, and J. M. Tour, Science **286**, 1550 (1999).

[32] M. di Ventra, S. T. Pantelides, and N. D. Lang, Phys. Rev. Lett. **84**, 979 (2000).
[33] J. G. Kushemerick, D. B. Holt, J. C. Yang, J. Naciri, M. H. Moore, and R. Shashidhar, Phys. Rev. Lett. **89**, 086802 (2002).
[34] H. Grabert and M. H. Devoret, in *Single Charge Tunneling*, edited by H. Grabert and M. H. Devoret, Vol. 294 of *NATO Advanced Study Institute, Series B: Physics* (Plenum, New York, 1992), Chap. 1.
[35] D. Porath, Y. Levi, M. Tarabiah, and O. Millo, Phys. Rev. B **56**, 9829 (1997).
[36] C. Kergueris, J. P. Bourgoin, S. Palacin, D. Esteve, C. Urbina, M. Magoga, and C. Joachim, Phys. Rev. B **59**, 12 505 (1999).
[37] S. N. Yaliraki, M. Kemp, and M. A. Ratner, J. Am. Chem. Soc. **121**, 3428 (1999).
[38] A. Nitzan, J. Phys. Chem. A **105**, 2677 (2001).
[39] A. Nitzan, Annu. Rev. Phys. Chem. **52**, 681 (2001).
[40] E. G. Petrov and P. Haenggi, Phys. Rev. Lett. **86**, 2862 (2001).
[41] X. D. Cui, A. Primak, X. Zarate, J. Tomfohr, O. F. Sankey, A. L. Moore, T. A. Moore, D. Gust, G. Harris, and S. M. Lindsay, Science **294**, 571 (2001).
[42] H. B. Weber, J. Reichert, F. Weigend, R. Ochs, D. Beckmann, M. Mayor, R. Ahlrichs, and H. Loehneysen, Chem. Phys. **281**, 113 (2002).
[43] V. Mujica, A. Nitzan, S. Datta, M. A. Ratner, and C. P. Kubiak, J. Phys. Chem. B **107**, 91 (2002).
[44] M. H. Hettler, H. Schoeller, and W. Wenzel, Europhys. Lett. **57**, 571577 (2002).
[45] B. Q. Xu and N. J. Tao, Science **301**, 1221 (2003).
[46] A. Nitzan and M. A. Ratner, Science **300**, 1384 (2003).
[47] Z. J. Donhauser, B. A. Mantooth, K. F. Kelly, L. A. Bumm, J. D. Monnell, J. J. Stapleton, D. W. Price, Jr., A. M. Rawlett, D. L. Allara, J. M. Tour, and P. S. Weiss, Science **292**, 2303 (2001).
[48] F. L. Carter, *Molecular Electronic Devices II* (Marcel Dekker, New York, 1987).
[49] J. S. Miller, Adv. Mater. (Weinheim, Ger.) **2**, 378 (1990).
[50] D. H. Waldeck and D. N. Beratan, Science **261**, 576 (1993).
[51] J. M. Tour, R. Wu, and J. S. Schumm, J. Am. Chem. Soc. **113**, 7064 (1991).
[52] W. Hu, H. Nakashima, K. Furukawa, Y. Kashimura, K. Ajito, and K. Torimitsu (unpublished).
[53] W. Wang, T. Lee, and M. A. Reed, Phys. Rev. B **68**, 035416 (2003).
[54] W. Franz, in *Handbuch der Physik*, edited by S. Flugge (Springer-Verlag, Berlin, 1956), Vol. 17, p. 155.
[55] C. Joachim and M. Magoga, Chem. Phys. **281**, 347 (2002).
[56] G. Lewicki and C. A. Mead, Phys. Rev. Lett. **16**, 939 (1966).
[57] J. G. Simmons, J. Appl. Phys. **34**, 1793 (1963).
[58] J. G. Simmons, J. Phys. D **4**, 613 (1971).